Sequence Analysis

PyroHMMvar: a sensitive and accurate method to call short IN-DELs and SNPs for Ion Torrent and 454 data

Feng Zeng[1], Rui Jiang[1,*] and Ting Chen[1,2,*]

[1]Bioinformatics Division, TNLIST/Department of Automation, Tsinghua University, Beijing 100084, China.

[2]Computational Biology and Bioinformatics Program, University of Southern California, Los Angeles, CA 90089, USA.

ABSTRACT

Motivation: The identification of short indels and SNPs from Ion Torrent and 454 reads is a challenging problem, essentially because these techniques are prone to sequence erroneously at homopolymers and can, therefore, raise indels in reads. Most of the existing mapping programs do not model homopolymer errors when aligning reads against the reference. The resulting alignments will then contain various kinds of mismatches and indels that confound the accurate determination of variant loci and alleles.

Results: To address these challenges, we realign reads against the reference using our previously proposed hidden Markov model (HMM) that models homopolymer errors and then merges these pairwise alignments into a weighted alignment graph. Based on our weighted alignment graph and HMM, we develop a method called PyroHMMvar which can simultaneously detect short indels and SNPs, as demonstrated in human resequencing data. Specifically, by applying our methods to simulated diploid datasets, we demonstrate that PyroHMMvar produces more accurate results than state-of-the-art methods, such as Samtools and GATK, and is less sensitive to mapping parameter settings than the other methods. We also apply PyroHMMvar to analyze one human whole genome resequencing dataset and the results confirm that PyroHMMvar predicts SNPs and indels accurately.

Availability and Implementation: Source code freely available at the following URL: https://code.google.com/p/pyrohmmvar/, implemented in C++ and supported on Linux.

Contact: tingchen@usc.edu, ruijiang@tsinghua.edu.cn

1 INTRODUCTION

The most prevalent variants on the human genome are single nucleotide polymorphisms (SNPs) (Abecasis, et al., 2012; Levy, et al., 2007; Wheeler, et al., 2008). The second most prevalent variants are insertions and deletions (indels) that occur every 7.2k base pairs (bp) (Mills, et al., 2006). Among them, more than 84% are short indels (<5bp) (Bhangale, et al., 2005). At present, the next generation sequencing technology facilitates the direct detection of SNPs and short indels by resequencing a personal genome (Nielsen, et al., 2011). After sequencing, reads are mapped against the refer-ence genome by read-mapping programs (Chen, et al., 2009; Homer, et al., 2009; Langmead and Salzberg, 2012; Li and Durbin, 2010; Li, et al., 2009; Ning, et al., 2001; Rumble, et al., 2009), and variants are called by hypothesis testing methods on the piled-up reads (DePristo, et al., 2011; Li, et al., 2008; Marth, et al., 1999). However, accurate variant detection depends on the ability to discriminate true variants from sequencing errors. Particularly, for Ion Torrent and 454 data, indels are the most common sequencing errors causing incorrect alignments and thus posing a major road-block to the accurate detection of variants. Ion Torrent and 454 can uniquely sequence homopolymers by quantifying the number of released by-products in the process of DNA synthesis (Margulies, et al., 2005; Rothberg, et al., 2011). At the same time, however, these techniques are prone to homopolymer sequencing errors, either overcalling or undercalling the number of homopolymer bases (Balzer, et al., 2010; Huse, et al., 2007). Moreover, the carry forward and incomplete extension (CAFIE) effects, which happen as a few template copies may grow in desynchronization with the population, also raise insertions in reads. However, existing mapping methods do not include models to tackle homopolymer errors; therefore, alignments around homopolymers can be incorrect, resulting in calling false variants (**Fig. 1**). Therefore, a comprehensive method is necessary to improve the accuracy of variant calling for Ion Torrent and 454 data.

Most of the existing methods detect SNPs and indels independently. The general strategy is to establish an accurate error model for the specific sequencing platform. For example, Atlas-SNP2 (Shen, et al., 2010) developed a logistical regression model relying on sequence context to discriminate true SNPs from sequencing errors. Realignment has been proven as an efficient method to improve accuracy by adjusting raw mappings. In response, Samtools (Li, et al., 2008), for example, deploys a concept termed Base Alignment Quality (BAQ) (Li, 2011) which is calculated by realigning a read against a reference to decrease false SNPs caused by nearby indels. Meanwhile, GATK (DePristo, et al., 2011) adjusts the alignments of reads spanning over indels by performing local multiple sequence alignment. However, as noted above, most of these methods are not designed to engage the problem of homopolymer errors and incorrect alignments around homopolymers. We previously proposed a method termed PyroHMMsnp (Zeng, et al., 2013) for Ion Torrent and 454. This

---

*To whom correspondence should be addressed: tingchen@usc.edu and ruijiang@tsinghua.edu.cn.
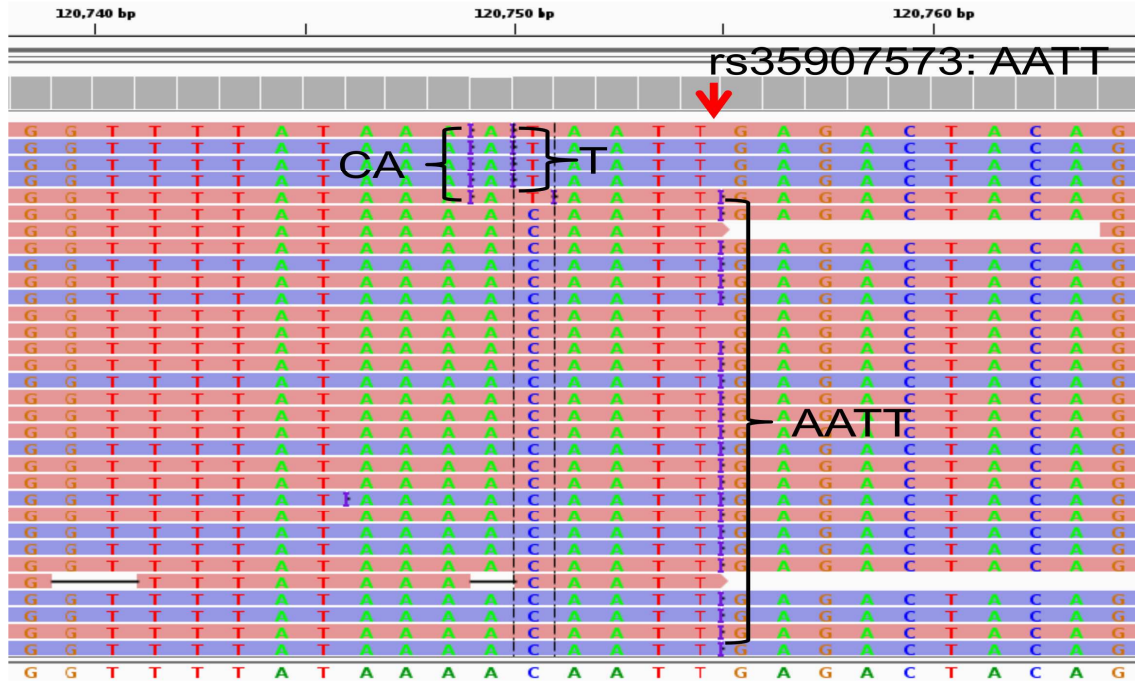
Fig. 1. Example of false alignments from 1000 Genome Project resequencing data. True variant is an insertion "AATT" at locus 120,754. Because that homopolymers "AAAA" in top five reads are sequenced to be "AAA", the read mapper produces false alignments. These false alignments will raise the false positive variants: a false insertion "CA" at locus 120,749 and a false SNP "C/T" at locus 120,750. If false alignments were adjusted correctly, these two false variants would not be called.

method implements a hidden Markov model (HMM) to formulate homopolymer errors and trains the HMM by an Expectation-Maximization (EM) algorithm using resequencing data. Then, the trained HMM is used to realign reads against the reference sequence around homopolymers to improve the performance of SNP calling.

Identification of insertions and deletions (indels) in the reference is a more challenging problem in short-read sequencing. One of the major obstacles is to identify potential genome positions where indels are located. Strategies for identifying insertions and deletions are different. Specifically, long insertions can only be found through sequence assembly, either local assembly (Li, et al., 2013) or global assembly (Iqbal, et al., 2012; Li, 2012), while deletions can be found through either sequence assembly or sequence alignments (Albers, et al., 2011; Emde, et al., 2012). Strategies for identifying short and long indels are also quite different. In principle, short indels, sometimes even long deletions, can be found by aligning one read against the reference, as long as a reliable read-mapping program is employed. However, because the read length is short, such mapping generally produces many false alignments with various kinds of indels and mismatches. To confirm the existence of an indel, we would have to examine multiple pieces of evidence, such as multiple aligned reads, read coverage, and constraints of paired-end reads. To the best of our knowledge, robust indel detection remains unsettled.

In this paper, we propose a method termed PyroHMMvar to call SNPs and short indels for both Ion Torrent and 454 resequencing data. Two distinct features are highlighted in PyroHMMvar. First,

we introduce a hidden Markov model (HMM) to formulate homopolymer errors. The HMM can accurately distinguish real signals from sequencing errors and thus improve the alignment of reads against the reference. The parameters of HMM are trained directly from raw mapping results through an iterative EM algorithm. Second, we propose a graph data structure which merges multiple aligned reads at a given locus into a weighted alignment graph from which we reconstruct the consensus sequence(s). The use of the weighted alignment graph provides the following advantages. First, it enables the straightforward construction of the haplotype(s) which may contain both SNPs and indels. In comparison, Dindel (Albers, et al., 2011) infers indels separately from SNPs. Second, we propose an efficient traversal algorithm over the weighted alignment graph to avoid the exhaustive and computationally complex enumeration of candidate haplotypes.

We simulate SNPs and short indels in the diploid genome and use them to test the performance of PyroHMMvar. Compared with two state-of-the-art methods, Samtools (Li, et al., 2008) and GATK (DePristo, et al., 2011), PyroHMMvar gives more accurate results. We also test the effect of the raw alignments produced by mapping programs to indel/SNP-calling accuracy by varying the scoring function of BWA-SW (Li and Durbin, 2010) to produce different mappings. The test results show that PyroHMMvar is less sensitive to the variation of the scoring function than the other programs. Finally, we apply PyroHMMvar to analyze one human whole genome resequencing dataset and the results confirms that PyroHMMvar predict SNPs and indels accurately.
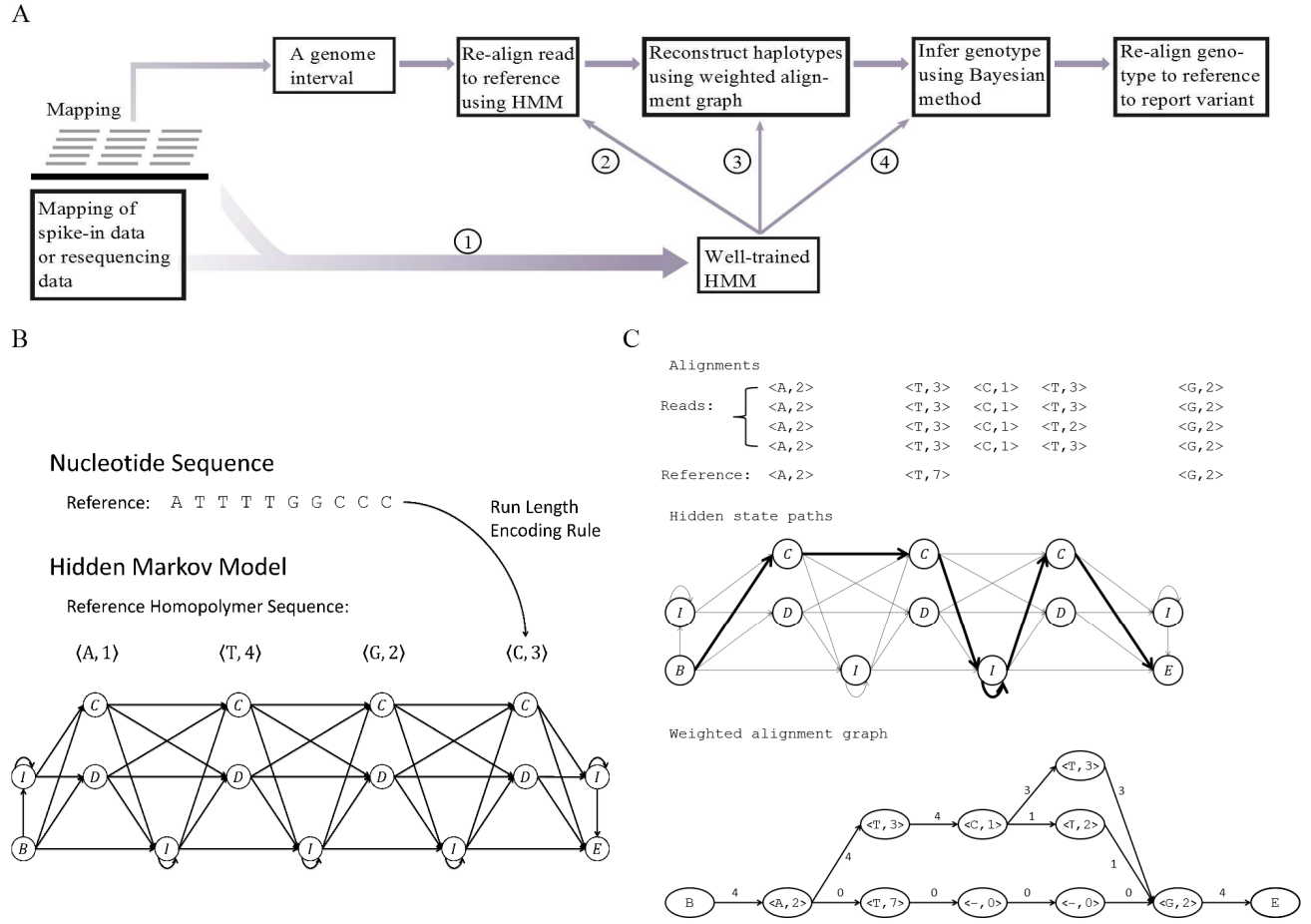
Fig. 2. (A) The schematic diagram depicts the workflow of PyroHMMvar. (B) The cartoon shows the topological structure of the HMM, the homopolymer sequence, and the hidden state transition. (C) An example of the weighted alignment graph that is established from the pairwise read-HMM alignments.

2 METHODS

As shown in **Figure 2A**, the workflow of PyroHMMvar includes the following steps. (1) We build and train an HMM model directly from the raw mapping of the resequencing data or the spike-in data using an iterative EM algorithm. (2) We use a sliding window to scan the genome. If the sliding window contains one or more candidate variants, we collect the short reads aligned within the sliding window and realign them against the reference using the HMM. (3) We then merge all the alignments (paths in HMM) to build a weighted alignment graph and traverse the graph to reconstruct the top candidate haplotypes. (4) Finally, we use a Bayesian method to infer the genotype from the set of candidate haplotypes and the short reads, followed by alignment of the genotype to the reference to determine the alleles and coordinates of variants. Details of these four steps are described in the following paragraphs.

2.1 Homopolymer hidden Markov model

An appropriate error model can facilitate the correct alignments of reads against the reference. We previously proposed a hidden Markov model (HMM, **Fig. 2B**) to formulate homopolymer sequencing errors in both Ion Torrent and 454 data(Zeng, et al., 2013). The HMM accepts a nucleotide sequence as input, and then converts the sequence into units of homopolymers using the Run Length Encoding Rule (Vacic, et al., 2008). As shown in **Fig 2B**, ATTTTGGCCCC becomes a sequence of 4 homopolymers <A,1><T,4><G,2><C,3>. For each homopolymer, there are two hidden states C and D. C means that the corresponding homopolymer is being sequenced while the length of the output homopolymer could be varying due to overcalling or undercalling errors. D represents that the homopolymer is not being sequenced in case that either the homopolymer may be deleted or the flow signal is too weak to be detected. A third hidden state I sitting between two consecutive homopolymers is used to model random insertions. Two hidden states $\{B, E\}$ are added into the model to represent the beginning and ending of the alignment because i) the quality at the beginning and ending of a read may be low, and ii) sometimes the exact boundaries (the beginning and ending) of the corresponding reference substring that produces the read are not clearly defined. Thus, the HMM model represents a local, rather than global, alignment. Based on the above notation, a hidden state π can take values from the set $\Pi = \{B, C, D, I, E\}$. For each read that is mapped to the reference, we use Viterbi's algorithm to compute a hidden state path $\boldsymbol{\pi} = \pi_1 \pi_2 \cdots \pi_n$, which represents a unique alignment between the read and the corresponding reference substring.

Hidden State Emission. In the above HMM, each hidden state can emit a homopolymer. Let $h = \langle \alpha, l \rangle$ represent the homopolymer input to a state π, and let $g = \langle \beta, k \rangle$ where $k \geq 0$ represent the homopolymer emitted by the state, where α, $\beta \in \{-, A, C, G, T\}$. However, in sequence comparison, we need a special homopolymer, a null homopolymer $\phi = \langle -, 0 \rangle$, to represent homopolymer indels. For a read homopolymer $g = \beta_1 \beta_2 \cdots \beta_k$, each compositional nucleotide β_i has a quality score q_i. We therefore define the quality score of the homopolymer as the average over the compositional nucleotides, as,

$$q_g = \frac{1}{k} \sum_{i=1}^{k} q_i. \tag{1}$$

Hence, the probability that state π emits output g given input h is modeled as,

$$p(g, q_g | h, \pi) = p(\beta | \alpha, \pi) p(k | \alpha, l, \pi) p(q_g | \alpha, l, \pi). \tag{2}$$

The base call rate $p(\beta | \alpha, \pi)$ represents the probability that an input base α is sequenced to an observed base β during nucleotide incorporation. The length call rate $p(k | \alpha, l, \pi)$ reflects the probability of observing k consecutive bases when a l bp homopolymer is given, and it is represented by a hierarchical model of the sequencing and base-calling procedures(Zeng, et al., 2013). $p(q_g | \alpha, l, \pi)$ formulates the quality score assigned by the base-calling procedure.

Parameter Estimation. To use the HMM to perform the realignment, the parameters of the HMM will be inferred from the following iterative EM algorithm. Parameters in the above HMM include the hidden state transition matrix, the base call rates, the length call rates, and the quality score distribution. The training data can be the resequencing data from one or more genomic loci, with no variants, or very few variants, or the spike-in data which are sequenced through the control lane of a sequencing platform to assess sequencing quality. The estimation of these parameters would be simple if the ground-truth alignments that represent the procedure of generating read sequences from templates were known. However, because the ground-truth alignments are not available, we propose an iterative strategy inspired by the EM algorithm (Dempster, et al., 1977) to train the HMM without the ground-truth alignments. In this strategy, the learning procedure is divided into two successive processes. First, given a read and its mapped reference sequence, the best alignment is computed and simultaneously assigned a posterior probability conditional on the previously learned parameters using the forward-backward algorithm (Durbin, et al., 1998). Next, occurrences of the state transitions and state emissions are counted from the probabilistically weighted alignments, and parameters of the HMM are updated according to the occurrences by using the maximum likelihood estimation (MLE). This procedure iterates until the likelihood value converges.

Pairwise Read-HMM alignment. After parameter estimation, the HMM is used to adjust a read mapping by realigning the read to the reference through the HMM. Given a read $\mathbf{r} = r_1 r_2 \cdots r_n$ and the corresponding reference sequence $\mathbf{t} = t_1 t_2 \cdots t_{m'}$ which is located through read-mapping, we first transform the reference $\mathbf{t}$ into homopolymer sequence $\mathbf{h} = h_1 h_2 \cdots h_m$, where $h_j = \langle \alpha_j, l_j \rangle$. Then, we apply the HMM to search for the optimal alignment between the read $\mathbf{r}$ and the template $\mathbf{h}$ using the Viterbi algorithm (Durbin, et al., 1998). We define the Viterbi variable $V(i, j, k, \pi)$ as the probability of the optimal alignment between the read prefix subse-

quence $\mathbf{r}_{[1:i]}$ and the homopolymer prefix subsequence $\mathbf{h}_{[1:j]}$ ending with the hidden state π, and, simultaneously, the suffix of $\mathbf{r}_{[1:i]}$ is a homopolymer of length k. We use the following recursion to calculate the Viterbi variable for $1 \leq i \leq n$, $1 \leq j \leq m$, as

$$
V(i, j, k, \pi) = \max_{i', j', k', \pi'} V(i', j', k', \pi') p(\pi | \pi')
$$
$$
p(\beta_i | \alpha_j, \pi) p(k_i | \alpha_j, l_j, \pi) p(q_g | \alpha_j, l_j, \pi), \tag{3}
$$

where $0 \leq i - i' \leq k_{max}$, $0 \leq j - j' \leq 1$, $0 \leq k' \leq k'_{max}$, $\pi' \in \Pi$, k_{max} is the maximum length of the homopolymer ended at read position i, k'_{max} is the maximum length of the homopolymer at read position i', and $p(\pi | \pi')$ is the transition probability between two states. Based on the recursion, we can use dynamic programming to compute the Viterbi variables, starting with the boundary conditions $V(0, 0, 0, B) = 1$ and $V(0, 0, 0, \pi) = 0$, where $\pi \neq B$, and ending with the Viterbi score $p(\mathbf{r}, \mathbf{h}, \boldsymbol{\pi}^*) = \max_k V(n, m, k, E)$.

2.2 Weighted alignment graph

Given all the pairwise read-reference alignments within a scanning window, we propose a graph data structure, termed weighted alignment graph, to merge all these alignments. Each read-reference alignment is represented by a path from B to E in the hidden space of the HMM (**Fig. 2C**). Stacking up all the paths in this window, we construct a weighted alignment graph, which is a directed acyclic graph with a starting node at the hidden state B and an ending node at the hidden state E. In this graph, the same hidden states and transition edges in multiple paths are merged and represented by one node and one directed edge, respectively. Each edge is weighted by the number of paths in which it appears. An example is shown in **Figure 2C**.

In this weighted alignment graph, a diploid genome should have one consensus path if the two underlying haplotypes are identical, or two different paths if the two underlying haplotypes are different. However, since each path in the graph represents a haplotype candidate, the number of paths grows exponentially by the number of branches in the graph. In regions where either the read quality or the alignment quality is low, the graph can be so complicated that an exhaustive search for all haplotype candidates is a computational burden. Fortunately, for most cases, true haplotypes correspond to paths with high weights in the graph. Therefore, we traverse the graph using a modified depth-first search (DFS) algorithm. For each node, we define an array to store the top k weighted paths from the starting node to this node. The algorithm consists of the following two steps:

1. Topological sort. We traverse the graph using the depth-first search (DFS) algorithm to produce a topological sort. The topological sort is a sorted order of the nodes from the left to the right such that every edge in the graph points from the left to the right. The topological sort takes $O(|V| + |E|)$ time, where $|V|$ is the number of nodes and $|E|$ is the number of edges.
2. Graph traversing. We traverse the nodes from the left to the right in the topological order. For each node, we compute the weights of all incoming paths, rank them, and store the top k weighted paths. The graph traversing takes $O(k|V| + k|E|)$ time.

This algorithm reduces the computational complexity.

2.3 Bayesian variant detection for diploid genome

We use the Bayesian method to infer the underlying genotype from the observed short reads and the candidate haplotypes generated by traversing the weighted alignment graph. Let $\mathbf{h}$ be a haplotype sequence. A read subsequence $\mathbf{r}_i \in R = \{\mathbf{r}_i | 1 \leq i \leq n\}$ is aligned against $\mathbf{h}$ by using the

Viterbi algorithm. The alignment score is used as the likelihood that **h** generates $\mathbf{r}_i$, as

$$p(\mathbf{r}_i|\mathbf{h}) = \max_{\boldsymbol{\pi}} p(\mathbf{r}_i, \boldsymbol{\pi}|\mathbf{h}). \tag{4}$$

The haplotype likelihood that **h** generates all read subsequences R is calculated by assuming that every read is sequenced from the haplotype independent of others, as

$$p(R|\mathbf{h}) = \prod_{i=1}^{n} \max_{\boldsymbol{\pi}} p(\mathbf{r}_i, \boldsymbol{\pi}|\mathbf{h}). \tag{5}$$

For diploid genome, the sequencing procedure can be considered as a two-stage model, shown in the following

$$\mathbf{g} \to \mathbf{h} \to \mathbf{r}. \tag{6}$$

At the first stage, a haplotype **h** is randomly sampled from the genotype $\mathbf{g} = \langle \mathbf{h}_1, \mathbf{h}_2 \rangle$. At the second stage, a read **r** is sequenced from the **h**. Based on the Bernoulli model, the genotype likelihood that **g** generates the data R is calculated by

$$p(R|\mathbf{g}) = \prod_{i=1}^{n} \left[p(\mathbf{h}_1|\mathbf{g}) p(\mathbf{r}_i|\mathbf{h}_1) + p(\mathbf{h}_2|\mathbf{g}) p(\mathbf{r}_i|\mathbf{h}_2) \right], \tag{7}$$

where by default $p(\mathbf{h}_1|\mathbf{g}) = p(\mathbf{h}_2|\mathbf{g}) = 0.5$. With genotype prior $p(\mathbf{g})$, the posterior that all reads are sequenced from **g** is computed by

$$p(\mathbf{g}|R) \propto p(R|\mathbf{g}) p(\mathbf{g}). \tag{8}$$

We use a multinomial distribution to model the prior of a haplotype pair $\mathbf{h}_1$ and $\mathbf{h}_2$. Let n_a be the length of the alignment between $\mathbf{h}_1$ and $\mathbf{h}_2$. Given the mismatch probability q_m and indel probability q_d, the prior probability of a genotype is defined as the probability that observing n_m mismatches and n_d indels in the alignment, calculated by,

$$p(\mathbf{g}) = \frac{n_a!}{(n_a - n_m - n_d)! n_m! n_d!} (1 - q_m - q_d)^{n_a - n_m - n_d} q_m^{n_m} q_d^{n_d}. \tag{9}$$

This prior setting is used to penalize a genotype of which two haplotypes are largely different from each other. The genotype $\mathbf{g}^*$ with the maximum posterior probability will be selected as the most possible underlying genotype.

A predicted variant is assigned a quality score, which is defined by how well the predicted variant explains the data. Specifically, a variant is of high quality if the best genotype explains the observed short reads well with the variant, but poorly without it. Therefore, the quality score for a variant v is defined as the following log-likelihood ratio:

$$Q_v = -10 \times \log \frac{\max_{g \in \bar{G}_v} p(g|R)}{\max_{g' \in G_v} p(g'|R) + \max_{g \in \bar{G}_v} p(g|R)}. \tag{10}$$

where G_v is the set of genotypes having the variant v, and $\bar{G}_v$ is the complement set of G_v.

The above proposed variant calling method works under the assumption of the reliable mappings, i.e., a read should be mapped back to the original genomic locus, at which there are a few false aligned positions or it is a correct alignment. However, this assumption cannot be guaranteed in practice. Therefore, we recalibrate the aforementioned variant quality score Q_v by integrating the mapping quality Q_m. The recalibrated variant

quality score is calculated as the geometric mean of the above quality scores,

$$Q = \sqrt{Q_v \times Q_m}. \tag{11}$$

where Q_m is defined as the median mapping quality score of short reads within the sliding window.

2.4 Aligning genotype with reference

The inferred genotype $\mathbf{g}^*$ contains the variant allele(s), but without such explicit information as a locus. For the example shown in **Figure 2C**, the haplotype sequence reconstructed by the weighted alignment graph gives two insertions <C,1><T,3> followed by a homopolymer sequencing error of undercalling. Therefore, to explicitly determine the variant(s), we use the standard dynamic programming for multiple sequence alignment to align the genotype against the reference. In our case, we have three sequences, including two haplotype sequences and one reference sequence, so the running time is $O(L^3)$ where L is the length of the sequences.

2.5 Computational complexity

The computational complexity of PyroHMMvar arises from two components. The first component is the pairwise read-HMM alignment. Suppose there are N reads of length w bp within a sliding window. The Viterbi algorithm, which is used to perform the pairwise alignment, achieves the time complexity $O(Nw^2)$. As a consequence of traversing the weighted alignment graph, k paths are generated as candidate haplotype sequences. N short reads are aligned pairwise against a candidate haplotype to calculate the data generation likelihood. Therefore, the computational complexity within a sliding window before we perform the Bayesian inference is $O(kNw^2)$. The second component is the alignment between the inferred genotype against the reference. This alignment is done through a standard dynamic programming for multiple sequence alignment. In our case, we have three sequences, including two haplotype sequences and one reference sequence; therefore, the running time is $O(w^3)$ where w is the length of the sequences. Hence, the total computational complexity within a sliding window is $O(kNw^2 + w^3)$. When PyroHMMvar is applied to a genome of size L bp, the complexity will be $O(\alpha(kNw^2 + w^3)) = O(kLNw + Lw^2)$, where $\alpha = L/w$ is the number of the sliding windows in the genome. To reduce the complexity, we use the banding technique to avoid the computation of the entire dynamic programming table for both the pairwise and multiple sequence alignment.

3 RESULTS

3.1 Data sets

We used two simulation datasets and one human whole genome resequencing data to compare the performance of PyroHMMvar with Samtools and GATK. We used the human chromosome 21 (chromosome size 48,129,895bp) to generate the first simulation data. We randomly chose 35,110 SNP sites (SNP rate 0.1%) and 4409 indel sites (indel rate 0.01%; indel size 1~5bp) on chromosome 21 to generate a pair of haplotypes. A variant site has a probability of 2/3 to be heterozygous and 1/3 to be homozygous. Next, we used the Ion Torrent simulator DWGSIG (https://github/com/nh13/dwgsim) to simulate the sequencing reads which are, on average, 400bp long with an error rate of 2%. Six datasets were generated by the simulator to assess the performance

Table 1. Performance evaluation of variant calling programs on the simulation of short reads generated from human chromosome 21 at various sequencing depths.

Depth	Method	SNP					INDEL					Runtime
		TP	FP	SEN[4]	SPE[5]	F_1	TP	FP	SEN	SPE	F_1	(Hour)
5x	PV[1]	15 739	**722**	**44.8%**	**95.6%**	**61.0%**	**838**	**37**	**19.0%**	**95.7%**	**31.7%**	0.53
	GA[2]	**15 740**	2 996	44.8%	84.0%	58.5%	759	52	17.2%	93.6%	29.1%	0.10[6]
	ST[3]	14 948	1 257	42.6%	92.2%	58.3%	745	993	16.9%	42.9%	24.2%	0.37
10x	PV	**28 393**	325	**80.9%**	**98.9%**	**89.0%**	**2 608**	92	**59.2%**	**96.6%**	**73.4%**	1.07
	GA	23 071	2 898	65.7%	88.8%	75.5%	2 467	101	56.0%	96.1%	70.7%	0.21
	ST	26 486	917	75.4%	96.7%	84.7%	1 741	1 340	39.5%	56.5%	46.5%	1.10
15x	PV	**32 757**	96	**93.3%**	**99.7%**	**96.4%**	**3 778**	80	**85.7%**	**97.9%**	**91.4%**	1.10
	GA	25 430	2 288	72.4%	91.7%	81.0%	3 672	157	83.3%	95.9%	89.1%	0.32
	ST	31 453	439	89.6%	98.6%	93.9%	2 466	1 528	55.9%	61.7%	58.7%	2.13
20x	PV	**34 202**	46	**97.4%**	**99.9%**	**98.6%**	**4 180**	69	**94.8%**	**98.4%**	**96.6%**	1.12
	GA	27 539	1 855	78.4%	93.7%	85.4%	4 124	174	93.5%	96.0%	94.7%	0.45
	ST	33 618	235	95.8%	99.3%	97.5%	2 904	1 566	65.9%	65.0%	65.4%	3.42
25x	PV	**34 681**	37	**98.8%**	**99.9%**	**99.3%**	**4 347**	70	**98.6%**	**98.4%**	**98.5%**	1.14
	GA	29 462	1 497	83.9%	95.2%	89.2%	4 302	179	97.6%	96.0%	96.8%	0.57
	ST	34 470	129	98.2%	99.6%	98.9%	3 238	1 748	73.4%	64.9%	68.9%	4.78
30x	PV	**34 861**	19	**99.3%**	**99.9%**	**99.6%**	**4 380**	52	**99.3%**	**98.8%**	**99.1%**	1.25
	GA	30 003	1 289	85.5%	95.9%	90.4%	4 345	161	98.5%	96.4%	97.5%	0.64
	ST	34 796	84	99.1%	99.8%	99.4%	3 418	1 765	77.5%	65.9%	71.3%	6.37

[1] PV is PyroHMMvar. [2] GA is GATK (v2.4-9). [3] ST is Samtools (v0.1.19). [4] *SEN* is Sensitivity. [5] *SPE* is Specificity. [6] The runtime of GATK is the runtime of IndelRealigner plus the runtime of UnifiedGenotyper.

of variant calling programs at the 5-, 10-, 15-, 20-, 25-, and 30-fold sequencing depths. The simulated short reads were mapped against human chromosome 21 by using the BWA-SW (Li and Durbin, 2010) with the default parameter setting.

The second simulation dataset was used to evaluate the effect of the mapping parameter setting on the performance of PyroHMMvar and other variant calling programs. Different parameter settings could produce different mappings and/or raw alignments of reads. We used the aforementioned simulation strategy to generate the sequencing reads (read length 400bp) with 10x depth from a 5Mbp segment on human chromosome 20 (Chr20:1000000 - 6000000). The simulated short reads were mapped against human chromosome 20 by using the BWA-SW with different mismatch penalties varying from 1 to 9.

We also applied PyroHMMvar and other variant calling programs to call SNPs and short indels in the human genome by using the whole genome resequencing data produced by an Ion Torrent PGM machine (NCBI Short Read Archive: ERX016676). The dataset consists of 859,757,279 reads, with an average length of 183bp at roughly 6x coverage.

3.2 Performance criteria

Three evaluation criteria were used: sensitivity, specificity, and F_1 score. Sensitivity is defined as the fraction of the annotated variants called by the program, specificity as the fraction of the called variants that are correct. Sensitivity measures the performance of a method in detecting true variants, and specificity assesses whether a method is capable of reporting few false positive variants. F_1 score is the harmonic mean of sensitivity and specificity. The formulas are shown in the following:

$$sensitivity = \frac{\#\{\text{True Positives}\}}{\#\{\text{Annotated variants}\}},$$

$$specificity = \frac{\#\{\text{True Positives}\}}{\#\{\text{Called variants}\}}, \tag{12}$$

$$F_1 = \frac{2 \times sensitivity \times specificity}{sensitivity + specificity}.$$
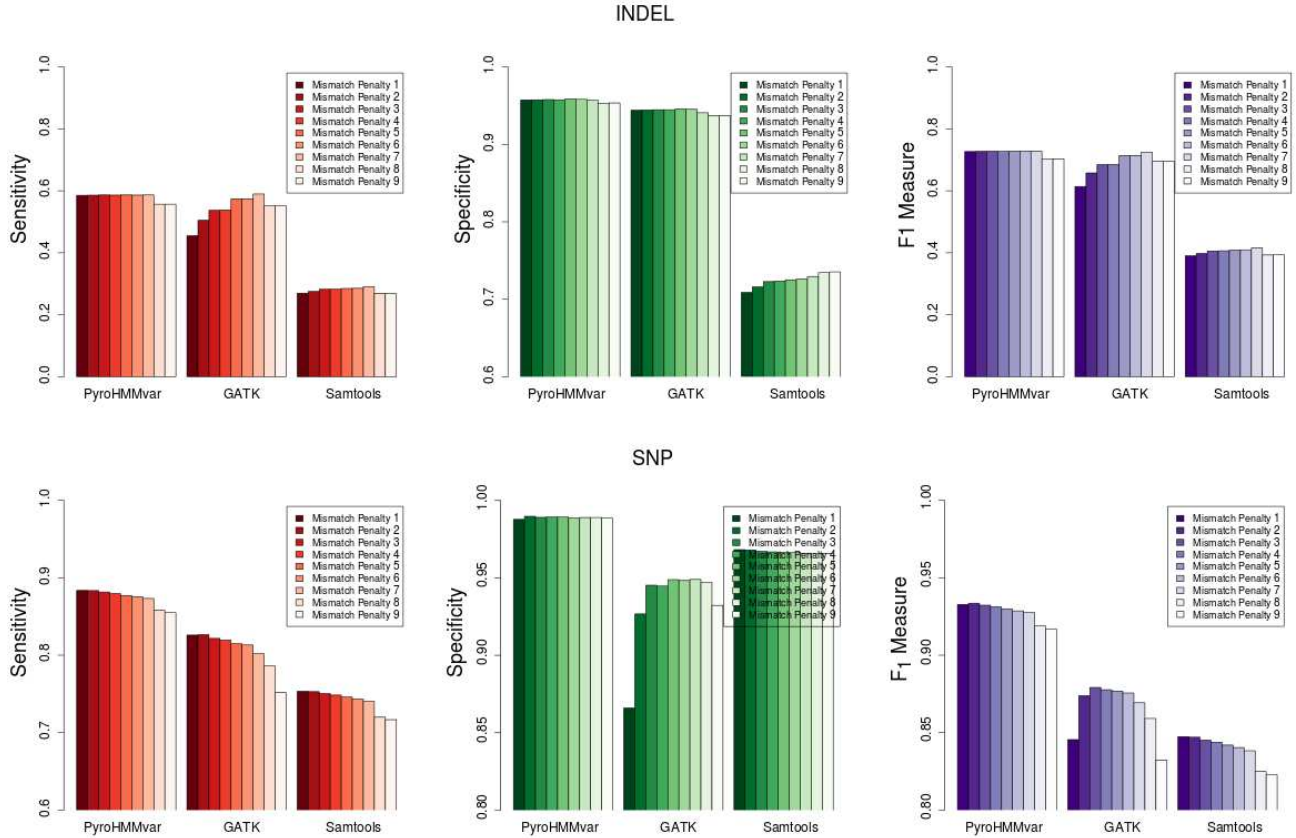
Fig. 3. Sensitivity, specificity, and F_1 measure when tuning the mismatch penalty from 1 to 9. Different scoring settings generate different mapping results, which then affect downstream variant calling. This figure shows the performance changes of three methods by using different penalty scores.

3.3 Diploid simulation with various sequencing depths

We used the DWGSIM simulator to generate six sets of sequencing reads from human chromosome 21 with varying coverage depths: 5x, 10x, 15x, 20x, 25x and 30x. PyroHMMvar, Samtools and GATK were applied to call SNPs and short indels. A called SNP is regarded as correct or true positive if the called locus is exactly the same as the simulated locus and the called genotype is concordant with the simulated genotype; otherwise, it is incorrect or false positive. An indel is regarded as a correct call if the called locus is within 5bp of the simulated locus, and the called genotype is concordant with the simulated genotype. These concepts, as applied to true and false positives, were applied to both SNPs and indels. A comparison of the performance of these three variant calling programs is shown in **Table 1**.

Across different coverages, PyroHMMvar called more true positive SNPs and fewer false positive SNPs, when compared to GATK and Samtools. For the high-coverage (30x depth) sequencing data, PyroHMMvar called 34,861 true positive SNPs, which implies a sensitivity of 99.3%, whereas GATK called 30,003 true positive SNPs (sensitivity 85.5%), and Samtools called 34,796 true positive SNPs (sensitivity 99.1%). Relative to its counterparts, PyroHMMvar called 16.2% more true positive SNPs than GATK and 0.2% more true positive SNPs than Samtools. Moreover, PyroHMMvar called only 19 false positive SNPs (99.9% specificity),

while GATK called 1289 false positive SNPs (95.9% specificity), and Samtools called 84 false positive SNPs (99.8% specificity). At the other sequencing depths, Samtools called slightly fewer true positive SNPs and slightly more false positive SNPs than PyroHMMvar. Overall, GATK predicted the fewest true positive SNPs and the most false positive SNPs at various sequencing depths. The results imply that PyroHMMvar and Samtools performed better in detecting SNPs than GATK in terms of both sensitivity and specificity.

The results also show that PyroHMMvar is accurate at detecting short indels. Overall, PyroHMMvar had the best performance in all three criteria (sensitivity, specificity and F_1) across all sequencing depths. PyroHMMvar predicted more simulated indels, as well as PyroHMMvar had the highest specificity. It is worth noting that the number of false positive indels called by PyroHMMvar decreases as the sequencing depth increases, whereas GATK and Samtools called more false positive indels along with the increase of sequencing depth. Across all sequencing data, the performance of Samtools' indel calling is well below that of PyroHMMvar and GATK. Overall, PyroHMMvar achieved the best performance in detecting both SNPs and short indels.

We also demonstrated the runtime of the three programs, which were performed at a single thread of a computer with a 3.4GHz CPU and 16 GB of memory. GATK achieved the fastest speed across all datasets. PyroHMMvar was slower than GATK, but

Table 2. Performance comparison of variant calling programs based on human whole genome resequencing data at the prediction accuracy >99.9% (variant quality score > 30).

Method	PyroHMMvar	GATK	Samtools
Total predicted SNPs	1 181 972	1 103 003	734 398
Validated (%)	1 173 633(99.3%)	1 093 986(99.2%)	731 859(99.7%)
Ts/Tv ratio[1]	2.17	2.18	2.19
Homozygous SNPs			
Predicted	687 985	752 994	597 993
Validated[2] (%)	687 278 (99.9%)	750 428 (99.7%)	597 195 (99.9%)
Heterozygous SNPs			
Predicted	493 987	350 009	136 405
Validated (%)	486 385 (98.5%)	343 558 (98.2%)	134 664 (98.7%)
Insertions			
Predicted	5 671	9 339	3 552
Validated (%)	5 583 (98.4%)	8 597 (92.6%)	3 266 (91.9%)
Deletions			
Predicted	19 304	101 602	11 530
Validated (%)	6 683 (34.6%)	13 510 (13.3%)	3 259 (28.3%)
Runtime (hour)	66.9	22.6[3]	36.4

[1] Ts/Tv ratio is the transition-to-transversion ratio. [2] The validation database is the dbSNP 137. [3] The runtime of GATK is the runtime of IndelRealigner plus the runtime of UnifiedGenotyper.

faster than Samtools. These three programs can all be accelerated by using the parallel computing technique.

3.4 Diploid simulation with varying scoring function

BWA-SW deploys a Smith-Waterman algorithm (Smith and Waterman, 1981) to perform local alignment of long reads. In general, different scoring functions will produce raw alignments, and may thus affect the performance of variant calling. Therefore, it is desirable that a variant calling method be less sensitive to the scoring function of the mapping programs in order to produce robust results. To assess this performance, we varied the mismatch penalty of BWA-SW from 1 to 9 and applied it to map the second simulated dataset at 10x depth. At a high mismatch penalty, the mapping program prefers indels over mismatches and produces different raw alignments. After applying PyroHMMvar, GATK, and Samtools to these datasets, we computed the sensitivity, specificity and F_1 measure, and the results are shown in **Figure 3**. Clearly, PyroHMMvar achieves consistent sensitivity and specificity across all parameter settings in detecting short indels. In contrast, the sensitivity of GATK increases when the mismatch penalty increases. We also noticed that the behavior of Samtools is different from other programs in that both the sensitivity and specificity increase as the mismatch penalty increases. This is because Samtools relies more on raw alignments to call indels.

Because the mapping program prefers indels over mismatches, the sensitivity in detecting SNPs decreases as the mismatch penalty increases. PyroHMMvar selects a variant locus as a SNP candidate when there are at least two reads supporting the variant. If the original mismatches are replaced by indels in the alignments, evidence is insufficient to support a variant locus as a candidate site. For the same reason, the sensitivity of SNP detection decreases in GATK and Samtools. However, while the specificity of PyroHMMvar and Samtools is consistent between them, the specificity of GATK is quite low at low mismatch penalty. Thus, with a small mismatch penalty, some indels appear like SNPs in the raw alignments, in turn causing GATK to call false positive SNPs. These results show that PyroHMMvar is more robust than the other tools.

3.5 Application to whole genome resequencing data

We downloaded a human whole genome resequencing dataset (NCBI SRA Accession: ERX016676), which was generated by an Ion Torrent PGM machine (Rothberg, et al., 2011). We used the BWA-SW to map the short reads back to the human reference hg19 with the default parameter setting and then applied the three variant calling programs to call SNPs and short indels. The called variants with a prediction error rate of higher than 0.1% (quality score <30) were eliminated. As demonstrated in **Table 2**, these results suggest that PyroHMMvar provides an accurate prediction of SNPs and short indels on human genome.

PyroHMMvar predicted 1,181,972 SNPs, among which 687,985 were homozygous and 493,987 were heterozygous. 99.9% of the predicted homozygous SNPs (687,278) and 98.5% of the predicted heterozygous SNPs (486,385) could be validated by the dbSNP 137. The predicted transition-to-transversion (Ts/Tv) ratio is 2.17. In comparison, GATK predicted less SNPs with a similar Ts/Tv ratio (2.18). The number of the predicted homozygous SNPs was larger (752,994), but the number of the predicted heterozygous SNPs was smaller (350,009). Their validation ratios are slightly lower than those of PyroHMMvar, at 99.7% for the homozygous SNPs and 98.2% for the heterozygous SNPs. Samtools made considerably fewer SNP predictions (734,398), but its validation ratios and Ts/Tv ratio are similar to the other two programs.

Table 3. The performance comparison of PyroHMMvar with PyroHMMvar-SW which replaces the HMM with a homopolymer-aware Smith-Waterman alignment method, and PyroHMMvar-Unique which uses the unique read sequences as the consensus sequences instead of the weighted alignment graph.

Method	SNP					INDEL				
	TP	FP	*SEN*	*SPE*	F_1	TP	FP	*SEN*	*SPE*	F_1
PyroHMMvar	28 393	325	80.9%	98.9%	89.0%	2 608	092	59.2%	96.6%	73.4%
PyroHMMvar-SW	28 297	340	80.6%	98.8%	88.8%	2 285	263	51.8%	89.7%	65.7%
PyroHMMvar-Unique	21 224	126	60.5%	99.4%	75.2%	1 723	018	39.1%	99.0%	56.0%

PyroHMMvar predicted 5,671 insertions for which the validation rate was 98.4%, and 19,304 deletions for which the validation rate was 34.6%. GATK called many more indels, but with lower validation rates: 9,339 insertions with 92.6% validation rate, and 101,602 deletions with 13.3% validation rate. Samtools predicted the fewest number of indels, only 3,552 insertions and 11,530 deletions. The validation rates of the insertions and deletions were 91.9% and 28.3%, respectively. The running times of PyroHMMvar, GATK and Samtools were 66.9, 22.6 and 36.4 hours, respectively.

3.6 The contribution of the HMM and the alignment graph in PyroHMMvar

To evaluate the contribution of the HMM in PyroHMMvar, we implemented a program, named PyroHMMvar-SW, which replaces the HMM by a homopolymer-aware Smith-Waterman alignment method, resembling PanGEA (Kofler, et al., 2009). In PyroHMMvar-SW, we assign a score +5 to a match and -3 to a mismatch. For an insertion or a deletion, we assign a score -4 to the gap opening penalty, and -1 to each gap extension penalty. For each pair of aligned homopolymers, in which a *k*-mer poly-nucleotide stretch is aligned to an *l*-mer poly-nucleotide stretch with identical nucleotide bases, we penalize the difference by -$1 \times |k$-$l|$ in the following scoring function,

$$s(k,l) = 5 \times \min(k,l) - 1 \times |k-l|. \quad (13)$$

We simulated a diploid genome sequencing data set with 10 fold sequencing coverage, and applied both PyroHMMvar and PyroHMMvar-SW to this data set. The results are shown in **Table 3.** Both programs show a similar performance in SNP calling, but the HMM clearly out-performs the Smith-Waterman method in the detection of insertions and deletions. PyroHMMvar called less false indels and achieved a higher specificity (96.6%) than PyroHMMvar-SW (89.7%). This improvement is due to the contribution of the HMM in modeling the homopolymer errors.

To evaluate the contribution of the weighted alignment graph method, we implemented a program called PyroHMMvar-Unique, which identifies potential haplotypes by using short reads instead of the weighted alignment graph and the DFS-based algorithm implemented in PyroHMMvar. Similarly, we simulated a diploid genome sequencing data set with 10 fold sequencing coverage, and applied both PyroHMMvar and PyroHMMvar-Unique to this data set. The results are shown in **Table 3**. PyroHMMvar has higher F_1 scores for both the SNP calling (89.0%) and the indel calling (73.4%) than PyroHMMvar-Unique (75.2% for the SNP calling

and 56.0% in the indel calling). This proves that the weighted alignment graph method significantly improve the performance of variant calling.

4 DISCUSSION

The Ion Torrent and 454 sequencing machines are the routine benchmark next-generation sequencing platforms with the leverage of affordable sequencing cost, low error rate and long read length. These sequencing machines are commonly used in microbiology and virology research. However, short reads generated by both Ion Torrent and 454 machines are contaminated by homopolymer errors, which invariably raise indels in data, thereby decreasing the accurate detection of SNPs and indels from resequencing data. In this paper, we introduced a computational framework which includes four components: (1) a hidden Markov model to model homopolymer errors; (2) a pairwise read-HMM realignment method by which scoring parameters are estimated from resequencing data; (3) a weighted alignment graph to reconstruct the underlying haplotype sequences; and (4) a Bayesian method to call the genotype. Based on the simulation experiments and application to real human whole genome resequencing data, the proposed realignment approach combined with the weighted alignment graph was demonstrated to be an effective strategy to increase the accurate detection of SNPs and short indels on both Ion Torrent and 454 resequencing data.

Although the method introduced in the paper is designed for Ion Torrent and 454 sequencing technologies, we believe that this computational framework conveys the following insights on the future development of variant calling method. Frist, it demonstrates a method of establishing an appropriate error model for a specific sequencing platform by 1) training the error model using the resequencing data and 2) applying the error model to realign the mappings. Second, it demonstrates the use of the alignment graph technique to reconstruct haplotype sequences. The alignment graph technique has also been shown to be effective in constructing high-quality consensus sequences from the long reads generated by the third-generation single molecular sequencing technology (Chin, et al., 2013). Furthermore, the alignment graph technique dramatically reduces the computational time of the otherwise exhaustive haplotype enumeration strategy, which was used in previously published works (Albers, et al., 2011; Zeng, et al., 2013). Overall, by replacing the homopolymer error model with an appropriate error model, the proposed computational framework can also benefit the detection of single nucleotide variants from resequencing data generated by other sequencing technologies, such as Illumina or Pacific Biosciences.

REFERENCES

Abecasis, G.R.*, et al.* (2012) An integrated map of genetic variation from 1,092 human genomes, *Nature*, **491**, 56-65.

Albers, C.A.*, et al.* (2011) Dindel: accurate indel calls from short-read data, *Genome research*, **21**, 961-973.

Balzer, S.*, et al.* (2010) Characteristics of 454 pyrosequencing data--enabling realistic simulation with flowsim, *Bioinformatics*, **26**, i420-425.

Bhangale, T.R.*, et al.* (2005) Comprehensive identification and characterization of diallelic insertion-deletion polymorphisms in 330 human candidate genes, *Human molecular genetics*, **14**, 59-69.

Chen, Y., Souaiaia, T. and Chen, T. (2009) PerM: efficient mapping of short sequencing reads with periodic full sensitive spaced seeds, *Bioinformatics*, **25**, 2514-2521.

Chin, C.S.*, et al.* (2013) Nonhybrid, finished microbial genome assemblies from long-read SMRT sequencing data, *Nature methods*, **10**, 563-569.

Dempster, A.P., Laird, N.M. and Rubin, D.B. (1977) Maximum Likelihood from Incomplete Data via the EM Algorithm, *Journal of the Royal Statistical Society. Series B (Methodological)*, **39**, 1-38.

DePristo, M.A.*, et al.* (2011) A framework for variation discovery and genotyping using next-generation DNA sequencing data, *Nature genetics*, **43**, 491-498.

Durbin, R.*, et al.* (1998) *Biological Sequence Analysis: Probabilistic Models of Proteins and Nucleic Acids*. Cambridge University Press.

Emde, A.K.*, et al.* (2012) Detecting genomic indel variants with exact breakpoints in single- and paired-end sequencing data using SplazerS, *Bioinformatics*, **28**, 619-627.

Homer, N., Merriman, B. and Nelson, S.F. (2009) BFAST: an alignment tool for large scale genome resequencing, *PloS one*, **4**, e7767.

Huse, S.M.*, et al.* (2007) Accuracy and quality of massively parallel DNA pyrosequencing, *Genome Biol*, **8**, R143.

Iqbal, Z.*, et al.* (2012) De novo assembly and genotyping of variants using colored de Bruijn graphs, *Nature genetics*, **44**, 226-232.

Kofler, R.*, et al.* (2009) PanGEA: Identification of allele specific gene expression using the 454 technology, *BMC Bioinformatics*, **10**, 143.

Langmead, B. and Salzberg, S.L. (2012) Fast gapped-read alignment with Bowtie 2, *Nature methods*, **9**, 357-359.

Levy, S.*, et al.* (2007) The diploid genome sequence of an individual human, *PLoS biology*, **5**, e254.

Li, H. (2011) Improving SNP discovery by base alignment quality, *Bioinformatics*, **27**, 1157-1158.

Li, H. (2012) Exploring single-sample SNP and INDEL calling with whole-genome de novo assembly, *Bioinformatics*, **28**, 1838-1844.

Li, H. and Durbin, R. (2010) Fast and accurate long-read alignment with Burrows-Wheeler transform, *Bioinformatics*, **26**, 589-595.

Li, H., Ruan, J. and Durbin, R. (2008) Mapping short DNA sequencing reads and calling variants using mapping quality scores, *Genome research*, **18**, 1851-1858.

Li, R.*, et al.* (2009) SOAP2: an improved ultrafast tool for short read alignment, *Bioinformatics*, **25**, 1966-1967.

Li, S.*, et al.* (2013) SOAPindel: Efficient identification of indels from short paired reads, *Genome research*, **23**, 195-200.

Margulies, M.*, et al.* (2005) Genome sequencing in microfabricated high-density picolitre reactors, *Nature*, **437**, 376-380.

Marth, G.T.*, et al.* (1999) A general approach to single-nucleotide polymorphism discovery, *Nature genetics*, **23**, 452-456.

Mills, R.E.*, et al.* (2006) An initial map of insertion and deletion (INDEL) variation in the human genome, *Genome research*, **16**, 1182-1190.

Nielsen, R.*, et al.* (2011) Genotype and SNP calling from next-generation sequencing data, *Nature reviews. Genetics*, **12**, 443-451.

Ning, Z., Cox, A.J. and Mullikin, J.C. (2001) SSAHA: a fast search method for large DNA databases, *Genome research*, **11**, 1725-1729.

Rothberg, J.M.*, et al.* (2011) An integrated semiconductor device enabling non-optical genome sequencing, *Nature*, **475**, 348-352.

Rumble, S.M.*, et al.* (2009) SHRiMP: accurate mapping of short color-space reads, *PLoS computational biology*, **5**, e1000386.

Shen, Y.*, et al.* (2010) A SNP discovery method to assess variant allele probability from next-generation resequencing data, *Genome research*, **20**, 273-280.

Smith, T.F. and Waterman, M.S. (1981) Identification of common molecular subsequences, *Journal of molecular biology*, **147**, 195-197.

Vacic, V.*, et al.* (2008) A probabilistic method for small RNA flowgram matching, *Pacific Symposium on Biocomputing. Pacific Symposium on Biocomputing*, 75-86.

Wheeler, D.A.*, et al.* (2008) The complete genome of an individual by massively parallel DNA sequencing, *Nature*, **452**, 872-876.

Zeng, F., Jiang, R. and Chen, T. (2013) PyroHMMsnp: an SNP caller for Ion Torrent and 454 sequencing data, *Nucleic Acids Res*, **41**, e136.